ELSEVIER

Journal of Alloys and Compounds 330–332 (2002) 229–233

Journal of ALLOYS AND COMPOUNDS

www.elsevier.com/locate/jallcom

Synchrotron powder diffraction line broadening analysis of dislocations in $LaNi_5$–H

E. Wu[a,*,1], E.MacA. Gray[a], D.J. Cookson[b,2]

[a]*School of Science, Griffith University, Brisbane 4111, Australia*

[b]*Australian National Beamline Facility, Photon Factory, KEK, Tsukuba, Ibaraki 305, Japan*

Abstract

In situ synchrotron powder diffraction data for the $LaNi_5$–H system were collected and the dislocation structures formed during the hydrogen activation cycle were studied by Rietveld refinement analysis in which anisotropic line broadening was modeled by dislocation scattering. Marginal line broadening was observed in the α phase formed by the very first hydrogen absorption by virgin metal. It is best modeled by dislocation $a/3\langle\bar{2}110\rangle$ on basal {0001} slip planes, with density 10^{10}–$10^{11}/cm^2$. In the β phase ($LaNi_5H_{\approx 6}$) and the activated α phase ($LaNi_5H_{\approx 0.4}$, postdesorption), in contrast, the majority of dislocations is prismatic with a {0110} slip plane and the same Burgers vector, with only a small proportion (~ 15%) of dislocations having basal slip planes. High dislocation densities of the order of $10^{12}/cm^2$ are associated with distributed strain fields of intermediate range. These results support the proposition that the dislocation structure is inheritable during the α–β phase transition, with the dislocations from the first-formed α phase on basal planes, and the majority created during nucleation and growth of the β phase on the prismatic planes, all being retained during subsequent phase transitions. © 2002 Published by Elsevier Science B.V.

Keywords: Synchrotron powder diffraction; Rietveld refinement; Dislocations; Anisotropic line broadening; $LaNi_5$

1. Introduction

It has been known for many years that the powder diffraction method can in principle provide information on dislocation structures [1–3]. It has only recently been shown that dislocation-induced anisotropic line broadening effects in diffraction patterns can be conveniently modeled as part of the Rietveld refinement process, and thereby provide invaluable information on the dislocation structure of the studied materials [4,5].

The first absorption of hydrogen by virgin $LaNi_5$ is a very complicated process, which involves the nucleation of the β phase, fracture and the introduction of large numbers of lattice defects into the alloy. This results in highly characteristic anisotropic diffraction peak broadening [6–8], in which (00*l*) peaks are narrowest while (*hk*0) peaks are broadest. These microscopic processes are manifested in a very large pressure hysteresis which decreases and becomes stable during the first several absorption–desorption cycles.

TEM examinations suggested that the principal defects are dislocations [9–11]. The X-ray orientation factor for the dislocation system $a/3\langle\bar{2}110\rangle\{0\bar{1}10\}$ is consistent with the anisotropic broadening observed in activated $LaNi_5$, and a preliminary analysis was successfully carried out to demonstrate the applicability of the Rietveld refinement method to dislocation studies [5].

In a recent study by Cerny et al. [12], the co-existence of a fraction (~10%) of a second type of dislocation system $a/3\langle\bar{2}110\rangle\{0001\}$ in activated $LaNi_5$ was also revealed from the analysis of high resolution synchrotron powder diffraction data. A recent study of the activation process by in situ neutron diffraction [8] has indicated that the absorption of hydrogen by virgin $LaNi_5$ (activation) occurs by a mechanism which is fundamentally different to that operating subsequently in activated materials. Therefore, we have studied the first hydrogen absorption–desorption cycle of $LaNi_5$ using the in situ synchrotron powder diffraction technique, and refined these high resolution data using the dislocation-induced anisotropic

*Corresponding author.

[1]Now at Department of Mechanical Engineering, University of Newcastle, Newcastle, NSW 2308, Australia.

[2]Now at ChemMat CARS Advanced Photon Source, Argonne, National Laboratory, Argonne, IL 60439-4859, USA.

0925-8388/02/$ – see front matter
PII: S0925-8388(01)01598-5

broadening model to obtain some detailed information about the dislocation structure developed during nucleation, hydrogen absorption and hydrogen desorption during the activation cycle.

2. Experimental procedure and analysis

$LaNi_5$ alloy (NUCOR Research Chemicals No. 1241 with a composition of $LaNi_{4.93}$) and ultrahigh purity hydrogen (up to 99.999%) purified and stored in a $LaNi_5$ reservoir were used.

The diffraction data were collected using BigDiff at the Australian National Beamline Facility at the Photon Factory of KEK in Tsukuba, Japan [13]. The beamline monochromator is a Si(111) channel-cut crystal located about 11 m from the synchrotron source. The diffractometer is a cylindrical cassette camera of radius 573 mm, accommodating imaging plates for rapid pattern collection. The resolution is classed as high.

About 10 mg of $LaNi_5$ powder sieved to <53 μm was loaded into an Al capillary sample holder (0.6 mm outer diameter, 0.3 mm inner diameter), rated to more than 30 bar pressure at 100°C. To enable continuous monitoring of the hydrogen pressure over the sample, a Sieverts-type hydrogenator was mounted within the camera cassette, on the diffractometer table. This permitted the sample to be rotated to achieve good powder averaging. The powder diffraction patterns were recorded on a set of two imaging plates covering the 2θ range $\pm5°$ to $\pm45°$. The imaging plates were exposed for 10 min with the cassette evacuated to ~0.1 Torr. High-resolution intensity vs. 2θ scans with 0.01° step size were extracted from the imaging plates using a BAS2000 image plate scanner.

Powder patterns were collected in situ at room temperature (21°C) for the $LaNi_5$ samples hydrogenated at various pressures (indicated as $P1$–$P9$) according to a previously measured pressure–composition phase diagram for activation of this particular $LaNi_5$ batch [7]. The hydrogenation was allowed to proceed for ~30 min for the reaction to reach quasiequilibrium before each diffraction measurement. The hydrogen-to-metal atomic ratio (H/M) at each pressure was determined by quantitative phase analysis, assuming hydrogen concentrations of $x=0.4$ and $x=6$ for α-and β-phase hydrides $LaNi_5H_x$, respectively. The diffraction pattern of the virgin $LaNi_5$ alloy in a 0.3-mm glass capillary was also recorded for reference (indicated as $P0$). The X-ray wavelength was determined to be 0.62649 Å from a standard NBS Si sample.

The crystal and dislocation structures were analysed using a customised version of the Rietveld program LHPM [14]. $LaNi_5$ and its α-phase hydrides were modeled in space group *P6/mmm*. The β phase was modeled in space group *P31m*, which permits some displacement of the Ni atoms in the unit-cell [15]. No attempt was made to locate the weakly-scattering H atoms in the unit cell.

The anisotropic line broadening was analyzed as previously detailed [4,5] based on the theories of Krivoglaz et al. [1] and Wilkens [2]. The integral breadth β is related to the dislocation structure of the crystallites by $\beta^2 = \rho\chi f(M)\tan^2\theta$ [4], where ρ is the dislocation density, χ is the X-ray orientation factor for the dislocation slip system [3,4], $f(M)$ is a function of the dimensionless dislocation distribution parameter M, which is in turn given by $M = r_c\rho$ (where r_c is the outer cut-off radius of the dislocation strain field) and is strongly related to the shape of the diffraction peak [2,4]. With the aid of the peak shape parameter, $y = \beta_L/\pi^{1/2}\beta_G$, where β_L and β_G are the integral breadths of the Lorentzian and Gaussian components of the Voigt function, the dislocation-induced broadening was modeled by refinable parameters related to the dislocation density (ρ) and dislocation structure (χ and M) in the crystallites [4,5]. The instrumental breadth parameters for the diffractometer were obtained by refinement of the standard Si powder pattern used for the wavelength calibration. With dislocation scattering now contributing to the Lorentzian breadth, the crystallite (domain) size broadening (expected to be Lorentzian) appeared to be small, so it was fixed at the value derived from the reference $LaNi_5$ ($P0$). For a given dislocation system, the program calculates the *hkl* dependence of χ, and defines the associated broadening of each reflection. The possibility of having a mixture of two types of straight dislocation slip systems for χ in each phase was incorporated into the program to deal with more complicated dislocation configurations such as that suggested by Cerny et al. [12].

To account for the Al peaks from the sample cell, and their extended tails, without losing intensity contributed by neighbouring $LaNi_5$ reflections, the intensities of the Al peaks were fitted regardless of the Al structure during the refinements. By this means, values of the agreement index R_{wp} around 5% were obtained.

3. Results and discussion

The in situ synchrotron powder diffraction patterns collected at various pressures for the first absorption–desorption cycle of $LaNi_5$ are shown in Fig. 1. The results of the subsequent line broadening analysis, including calculated dislocation densities and structures, are summarised in Table 1. The atomic coordinates derived from the refinements have not been included, since these were consistent with literature values, and are not the main concern in this study. The refined profiles of two selected synchrotron diffraction patterns are presented in Fig. 2. The calculated lattice parameters of each phase at different pressures are displayed in Fig. 3.

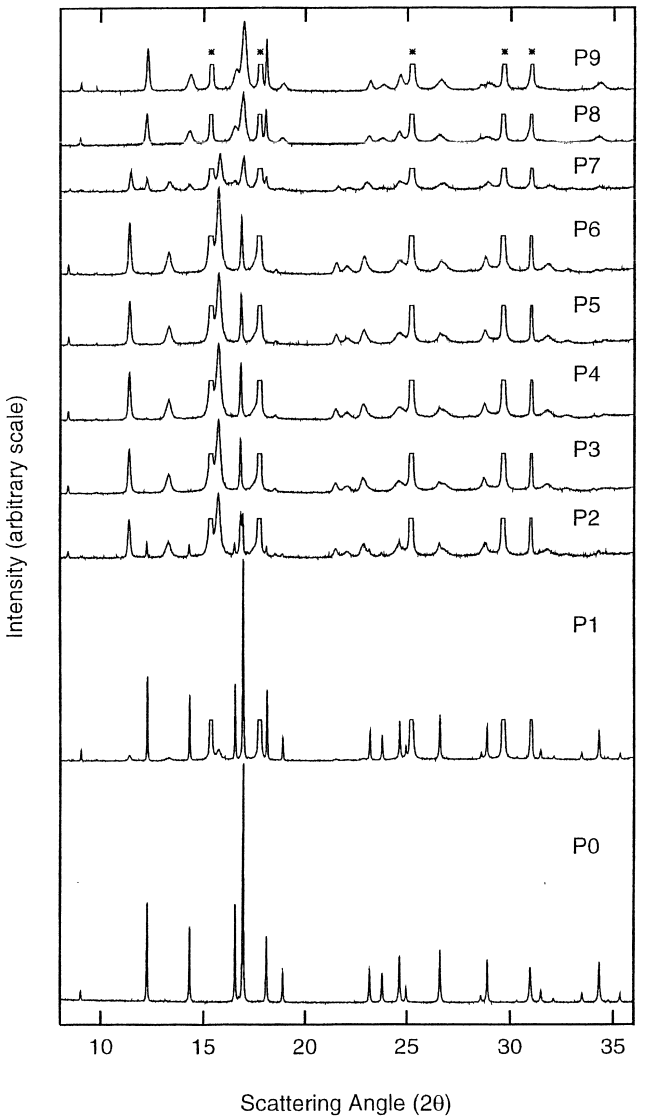

Fig. 1. In situ synchrotron powder diffraction patterns collected at pressures detailed in Table 1 during the first hydrogen absorption–desorption cycle of $LaNi_5$. Reflections marked with * are from that of Al sample holder and have been cut to the sample reflection level.

According to Table 1, the diffraction patterns can roughly be divided into four regions. *P*1 and *P*2 are in the two-phase region of the absorption plateau; *P*3, *P*4, *P*5 are in the pure β-phase region of desorption. *P*6, with <1% of α phase present, is at the boundary of the two-phase region and so belongs with *P*3–*P*5. *P*7 is in the two-phase region of the desorption plateau. *P*8 and *P*9 are in the pure α-phase region of the desorption isotherm.

At *P*1 (560 kPa) the sample is ~20% β phase, so the predominant phase remains 'preactivated' α phase. There is very little broadening and not much anisotropy in this form of the α phase. However, the high resolution of the diffractometer permits analysis, and the weak anisotropic broadening can be described by edge dislocations $a/3\langle\bar{2}110\rangle$ on basal slip planes {0001} with density $\sim 1\times 10^{10}/\mathrm{cm}^2$, associated with a moderate strain field ($M\sim 1.3$). The agreement of this model is marginally better than an isotropic broadening approach (of unspecified origin) and models containing other dislocation systems. At the next-highest pressure (*P*2), the α phase is present as a small fraction (14%), but the broadening can still be assessed as arising in the same dislocation structure but with a short-ranged strain field ($M\sim 0.3$) and a high dislocation density ($\sim 3\times 10^{11}/\mathrm{cm}^2$). Though sharing the same Burgers vector $a/3\langle\bar{2}110\rangle$, this dislocation structure is qualitatively different from that in fully activated $LaNi_5$ (dislocation predominantly on $\{0\bar{1}10\}$ planes) reported previously [5,12]. This new result in fact agrees with the observations of {0001} slip planes in the α phase during TEM examinations [11].

The development of the β phase in the two-phase region (*P*1 and *P*2) follows an opposite trend, with only a small proportion (~ 15%) of $a/3\langle\bar{2}110\rangle$ dislocations on the basal plane, and the majority on prismatic planes. This suggests that the nucleation of β-phase precipitates preserves the dislocation structure on basal planes from the parent α phase, but growth occurs preferentially on prismatic planes. Very high dislocation densities were calculated for the β-phase in the two phase region, though these must be regarded as only indicative owing to the difficulty of estimating dislocation density from peaks with low *M* values [4]. However, the low *M* values do reflect a higher Lorentzian contribution to the peaks, suggesting that relatively short-ranged strain fields have been built up around the α–β phase interface due to the lattice misfit between the two phases. The misfit around β-phase precipitates appears to have only a minor effect on the α phase when the α phase predominates near the α/α–β-phase boundary, as indicated by the low dislocation density and anisotropic lattice expansion of the unit cell at *P*1 (see Fig. 3). This agrees with the incoherent nature of the interface in this region deduced from lattice parameter measurements [8], and could help to explain the significantly larger pressure hysteresis in the initial absorption–desorption cycle (e.g. [7]). However, the α phase near the α–β/β-phase boundary (*P*2) appears to have been affected by the misfit, generating a high density of dislocations and isotropic expansion of both *a* and *c* axes, indicating that the interface could become coherent at the β-phase end the two-phase region [16]. This is readily understood as a result of the diminution of the size of the α-phase particles as β-phase fragments form and separate by fracture or spallation [8]: eventually, the particles will be small enough for some strain relaxation to occur, leading to partial lattice coherency.

At higher pressure (*P*3, 1300 kPa), the sample becomes pure β-phase hydride. Here the dislocation structure is similar to that in the *P*2 state near the α–β/β-phase boundary. In the next three steps (*P*4, *P*5 and *P*6) of

Table 1
Dislocation structures derived from in situ synchrotron powder diffraction line broadening analysis

Sample conditions	Dislocation configurations
*P*0: Virgin powder	$\epsilon_{rms}=0.06\%$, $D=400(10)$ nm
*P*1: Absorption $P=560$ kPa	α-phase: 81.2% $a_\alpha/3\langle\bar{2}110\rangle\{0001\}$ $M=1.3$; $\rho=1.2\times10^{10}/cm^2$ β-phase: 18.8% $a_\beta/3\langle\bar{2}110\rangle\{0\bar{1}10\}$ 86%; $a_\beta/3\langle\bar{2}110\rangle\{0001\}$ 14% $M\sim0.3$; $\rho\sim9\times10^{12}/cm^{2a}$
*P*2: Absorption $P=890$ kPa	β-phase: 85.9% $a_\beta/3\langle\bar{2}110\rangle\{0\bar{1}10\}$ 84%; $a_\beta/3\langle\bar{2}110\rangle\{0001\}$ 16% $M\sim0.8$, $\rho\sim2\times10^{12}/cm^2$ α-phase: 14.1% $a_\alpha/3\langle\bar{2}110\rangle\{0001\}$ $M\sim0.4$; $\rho\sim3\times10^{11}/cm^{2a}$
*P*3: Absorption $P=1300$ kPa	β-phase: $a_\beta/3\langle\bar{2}110\rangle\{0\bar{1}10\}$ 85%; $a_\beta/3\langle\bar{2}110\rangle\{0001\}$ 15% $M=0.9$; $\rho=1.6\times10^{12}/cm^2$
*P*4: Desorption $P=880$ kPa	β-phase: $a_\beta/3\langle\bar{2}110\rangle\{0\bar{1}10\}$ 86%; $a_\beta/3\langle\bar{2}110\rangle\{0001\}$ 14% $M=0.8$; $\rho=2.0\times10^{12}/cm^2$
*P*5: Desorption $P=600$ kPa	β-phase: $a_\beta/3\langle\bar{2}110\rangle\{0\bar{1}10\}$ 85%; $a_\beta/3\langle\bar{2}110\rangle\{0001\}$ 15% $M=0.7$; $\rho=2.0\times10^{12}/cm^2$
*P*6: Desorption $P=320$ kPa	β-phase: $a_\beta/3\langle\bar{2}110\rangle\{0\bar{1}10\}$ 81%; $a_\beta/3\langle\bar{2}110\rangle\{0001\}$ 19% $M=0.7$; $\rho=2.0\times10^{12}/cm^2$
*P*7: Desorption $P=140$ kPa (assuming zero coherency strain)	β-phase: 63.7% $a_\beta/3\langle\bar{2}110\rangle\{0\bar{1}10\}$ 79%; $a_\beta/3\langle\bar{2}110\rangle\{0001\}$ 21% $M\sim0.2$, $\rho\sim2\times10^{13}/cm^{2a}$ α-phase: 36.3% $a_\alpha/3\langle\bar{2}110\rangle\{0\bar{1}10\}$ 87%; $a_\alpha/3\langle\bar{2}110\rangle\{0001\}$ 13% $M\sim0.6$, $\rho\sim3\times10^{12}/cm^2$
*P*8: Desorption $P=60$ kPa	α-phase: $a_\alpha/3\langle\bar{2}110\rangle\{0\bar{1}10\}$ 85%; $a_\alpha/3\langle\bar{2}110\rangle\{0001\}$ 15% $M=1.0$; $\rho=1.4\times10^{12}/cm^2$
*P*9: Desorption Vacuum, $P\sim1$ kPa	α-phase: $a_\alpha/3\langle\bar{2}110\rangle\{0\bar{1}10\}$ 89%; $a_\alpha/3\langle\bar{2}110\rangle\{0001\}$11% $M=1.3$; $\rho=1.1\times10^{12}/cm^2$

[a] The value of the calculated dislocation density is only indicative.

desorption down to the β/β+α phase boundary at 320 kPa, the dislocation densities are very similar, and essentially independent of hydrogen content and lattice parameters (Fig. 3). However there is a slight increase in the Lorentzian component (indicated by the value of *M*), suggesting a shorter-ranged strain field and a slightly relaxed dislocation distribution.

In the *P*7 state (desorption, 140 kPa), 40% α phase and 60% β phase co-exist. The same type of dislocation structure (Table 1) was used to model the broadening in both phases in this region. As found in the *P*1 and *P*2 conditions, the predominantly Lorentzian profile of the strongly broadened peaks suggests high dislocation densities and short-ranged strain fields. In this condition, however, the α and β phases interact mechanically [17], so some of the strain broadening must come from lattice parameter misfit at the now partially coherent α-β interface.

Further desorption (*P*8 at 60 kPa and *P*9 in vacuum) recovers the pure α phase. The dislocation structure is however quite different from that in the preactivated α phase and practically identical to that of the β phase. Thus the β-phase dislocation structure appears to survive the reverse phase transition to be inherited by the α phase. The dislocation analysis of the dehydrided metal confirmed the dislocation structure derived by Cerny et al [12], who found about 90% of dislocations on prismatic planes and 10% on basal planes, although their total calculated dislocation density was lower ($\sim10^{11}/cm^2$) than we obtained. An error in the Burgers vector for $LaNi_5$ resulting in higher calculated dislocation density in [5] has been corrected in this work. However, the discrepancy between this work and Cerny et al.,'s [12] is still relatively high, though the measured line broadening in both appears to be the same. The latest TEM study of activated $LaNi_5$ [18] produced density estimates above $10^{12}/cm^2$.

4. Conclusions

The combination of in situ synchrotron powder diffraction with Rietveld profile analysis implementing a dislocation-induced line broadening model have elucidated the dislocation structures formed in $LaNi_5$ and its α-and β-hydrides during the first hydrogenation–dehydrogenation cycle.

Dislocations $a/3\langle\bar{2}110\rangle$ on basal planes were found in the preactivated α phase. Our results suggest that, while

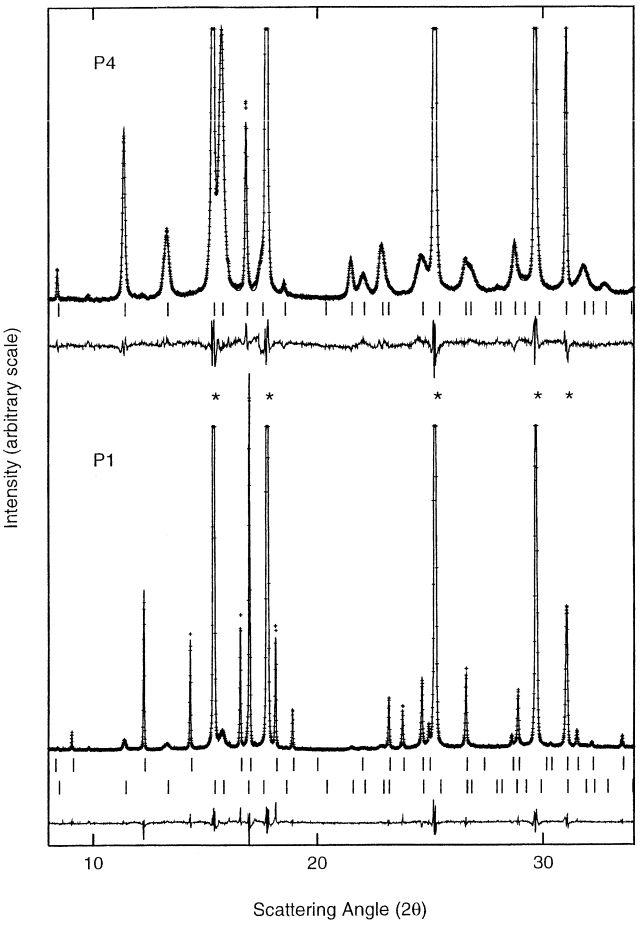

Fig. 2. Rietveld refinement results obtained by applying the dislocation-induced broadening model to two sets of diffraction data: the α and β phases during hydrogen activation of virgin metal at 560 kPa (*P*1), and the pure β phase at 880 kPa (*P*4). The difference profiles for the refinement along with the reflection markers for the α phase (top) and the β phase (bottom) are shown below. The reflections from the Al sample holder were also refined.

incoherent initially, the phase transition in virgin metal may become partially coherent near the α+β/β phase boundary.

The similarity of the dislocation structures found in the β phase and subsequently in the activated α phase suggests that dislocation defects survive the phase transition and are thus inheritable.

Acknowledgements

The authors thank the Australian Research Council and the Australian Synchrotron Research Program for their support. We are grateful to Dr E.H. Kisi (University of Newcastle) for helpful discussions of several aspects of this work.

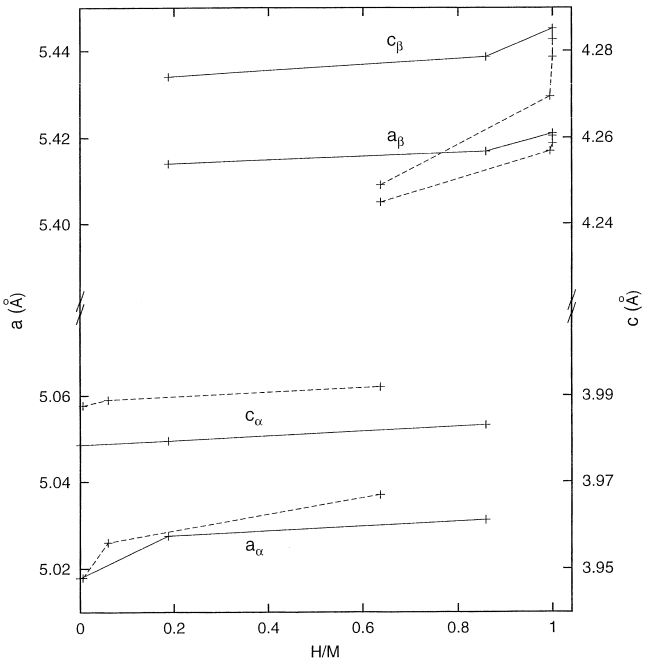

Fig. 3. Measured lattice parameters of each phase at the various pressures noted in Table 1 during absorption (solid lines) and desorption (dashed lines).

References

[1] M.A. Krivoglaz, K.P. Ryaboshapka, Fiz. Metall. Metallov. 15 (1963) 18.
[2] M. Wilkens, Phys. Stat. Sol. (a) 2 (1970) 359.
[3] P. Klimanek, R. Jr Kuzel, J. Appl. Cryst. 21 (1988) 59.
[4] E. Wu, E.Mac.A. Gray, E.H. Kisi, J. Appl. Cryst. 31 (1998) 356.
[5] E. Wu, E.H. Kisi, E.MacA. Gray, J. Appl. Cryst. 31 (1998) 363.
[6] K. Nomura, H. Uruno, S. Ono, H. Shimozuka, S. Suda, J. Less-Common Met. 107 (1985) 221.
[7] E.H. Kisi, C.E. Buckley, E.MacA. Gray, J. Alloys Comp. 185 (1992) 369.
[8] M.P. Pitt, E.MacA. Gray, E.H. Kisi, B.A. Hunter, J. Alloys Comp. 293–295 (1999) 118.
[9] E.H. Kisi, M.J. Goringe, P.S. Turner, E.MacA. Gray, Z. Phys. Chem. 181 (1994) 1141.
[10] G.H. Kim, C.H. Chun, S.G. Lee, J.Y. Lee, Acta Metall. Mater. 42 (1994) 3157.
[11] G.H. Kim, S.G. Lee, K.Y. Lee, C.H. Chun, J.Y. Lee, Acta Metall. Mater. 43 (1995) 2233.
[12] R. Cerny, J.-M. Joubert, M. Latroche, A. Percheron-Guegan, K. Yvon, J. Appl. Cryst. 33 (2000) 997.
[13] T.M. Sabine, B.J. Kennedy, R.F. Garrett, G.J. Foran, D.J. Cookson, J. Appl. Cryst. 28 (1995) 513.
[14] B.A. Hunter, C.J. Howard, Rep. AAEC/M112, Australian Atomic Energy Commission, Lucas Heights, 1995.
[15] P. Fischer, A. Furrer, G. Busch, L. Schlapbach, Helvet. Phys. Acta 50 (1977) 421.
[16] H.K. Birnbaum, J. Less-Common Met. 104 (1984) 31.
[17] E.H. Kisi, E.MacA. Gray, S.J. Kennedy, J. Alloys Comp. 216 (1994) 123.
[18] H. Inui, T. Yammamoto, M. Hirota, M. Yamaguchi, Lattice defects introduced during hydrogen absorption–desorption cycles and their effects on *PCT* characteristics in some intermetallic compounds, in press.